RSC Advances

ROYAL SOCIETY OF CHEMISTRY

www.rsc.org/advances

Mechanistic Insight in Phase Transfer Agent Assisted Ultrasonic Desulfurization

Jaykumar B. Bhasarkar[1], Mohit Singh[2], Vijayanand S. Moholkar[1,*]

[1] Department of Chemical Engineering, Indian Institute of Technology Guwahati, Guwahati – 781039, Assam, India

[2] Department of Chemical Engineering, National Institute of Technology Tiruchirapalli, Tiruchirapalli – 620015, Tamil Nadu, India

* Corresponding author. E–mail: vmoholkar@iitg.ernet.in, Fax: +91 361 258 2291

ABSTRACT

This paper attempts to gain physical insight into the phase transfer agent (PTA) assisted ultrasonic oxidative desulfurization process. Essentially, the synergistic links between mechanisms of PTA and ultrasound/ cavitation have been identified by coupling experimental results with simulations of cavitation bubble dynamics and Arrhenius & thermodynamic analysis of reaction kinetics. It is revealed that ultrasonic oxidative desulfurization has radical–based mechanism with least activation energy. However, due to high instability of radicals, the frequency factor is small leading to low dibenzothiophene (DBT) oxidation. PTA–assisted oxidative desulfurization has ionic mechanism with much higher activation energy. The synergistic effect of fine emulsification generated by micro–convection due to ultrasound and cavitation, and PTA–assisted interphase transport of oxidant results in almost complete oxidation of DBT. It is thus established that synergy between mechanisms of ultrasound/ cavitation and PTA is predominantly of physical nature. Moreover, effect of PTA is more marked for ultrasonic system than mechanically agitated system.

Keywords: Oxidation, Desulfurization, Phase transfer agent, Ultrasound, Cavitation

1. Introduction

Stringent restrictions on sulfur content of the fuel to curb the pollution due to vehicular emission has triggered significant research on new technologies for achieving deep desulfurization of transportation fuels.[1] The conventional technology of hydro–desulfurization (HDS), in which the sulfur in the fuel is removed as H_2S, is not suitable for achieving very low levels of sulfur, as required. The principal cause contributing to this effect is low reactivity (and hence negligible removal) of substituted benzothiophene and dibenzothiophene.[2]

New technology of oxidative desulfurization has shown significant promise for achieving deep desulfurization. This technology is based on conversion of non–polar aromatic hydrocarbons containing sulfur to corresponding sulfones, which can subsequently be extracted from fuel. Oxidants used in this technique are organic or inorganic peroxyacids, which are immiscible with the fuel. Thus, the oxidative desulfurization reaction system is essentially liquid–liquid heterogeneous system, which is limited by mass transfer. Kinetics as well as yield of such system depends on the interfacial area between the two phases. Ultrasound irradiation (or sonication) is a well–known technique for enhancing the interphase mass transfer in diverse physical and chemical processes through generation of strong micro–convection.[3-6] Transient cavitation also generates highly reactive radicals through thermal dissociation of solvent vapor entrapped in the cavitation bubble at the moment of collapse. Another means of enhancing the interfacial mass transfer in a liquid–liquid heterogeneous system is the use of phase transfer catalyst or phase transfer agent (PTA).[7] PTA enhances interphase mass transfer by formation of complex with the nucleophilic reagent in aqueous phase (or the oxidant in context of present study), and transport of the complex to the organic phase. Simultaneous application of ultrasound and PTA for oxidation desulfurization has been attempted by several authors.[8–10] Hagenson et al.[11] and Hagenson and Doraiswamy[12] have analyzed the effect of ultrasound, phase transfer agent and microphase in enhancement of synthesis of benzyl sulfide from benzyl chloride and sodium sulfide. Ultrasound was revealed to enhance intrinsic mass transfer as well

as effective diffusivity of the organic reactant through the product layer. Ultrasound was revealed to boost the effects of microphase and PTA on enhancement of reaction kinetics. This was attributed to enhancement of interphase mass transfer due to strong micro–convection generated by ultrasound.

Most of the research in ultrasound–assisted oxidative desulfurization has focused on results than rationale. The physical mechanism of this process has remained largely unexplored. In a previous paper, we have attempted to identify the physical mechanism of ultrasound assisted oxidative desulfurization by distinguishing between individual effects of ultrasound and cavitation on the reaction system. We demonstrated that generation of reducing species such as H_2, CO and CH_4 during transient cavitation in organic phase hinders oxidation of sulfur compounds due to competitive consumption of oxidant species.[13,14] In another paper, we explored the effect of PTA on oxidative desulfurization using different peracid oxidant systems (performic acid and peracetic acid). In this study we showed that interfacial transport of oxidant in the form of oxidant–PTA complex reduces the undesirable consumption of oxidant by reducing species, as observed in our earlier study.[15] Although this paper demonstrated the beneficial effect of PTA on ultrasonic oxidative desulfurization system, underlying physical mechanism was not established. In the present study, we have attempted to identify the physical mechanism of the PTA–assisted ultrasonic oxidative desulfurization process. Our approach is based on determination of the kinetic (Arrhenius) and thermodynamic parameters of oxidative desulfurization in different experimental categories, and its concurrent analysis with simulation of cavitation bubble dynamics. For the kinetic analysis of PTA–assisted oxidative desulfurization, we have used the model of Zhao et al.[16] The principal objectives of this study are two–fold: (1) assessment of the relative contributions of ultrasound and PTA to enhancement of oxidative desulfurization, and (2) determination of the relative influence of interfacial mass transfer and intrinsic reaction kinetics in the process.

2. Materials and Methods

2.1 Chemicals: The following chemicals have been used in the experiments: Dibenzothiophene (98% from Sigma Aldrich), toluene (Synthesis grade from Merck), 30% v/v H_2O_2 (AR grade from Merck), formic acid (~ 86%, AR grade from Lobachem), tetrabutyl ammonium bromide (TBAB) (from Sigma Aldrich), acetonitrile (HPLC grade from Merck). All chemicals were used as received without any pretreatment.

2.2 Experimental setup: Experiments were conducted in an ultrasound bath (Make: Jeio–Tech, Model: UC02, Capacity: 2 L, Frequency: 35 kHz, Power: 70 W). The actual power dissipated in the bath was determined calorimetrically, and the acoustic pressure amplitude generated in the bath was calculated as 150 kPa.[17] Oxidative desulfurization reactions were carried out in 38 mL test tube, which was placed at the center of the bath. Due to spatial variations of ultrasound intensity in the bath, the position of the test tube inside bath was carefully kept constant in all experiments.[18] For determination of activation energy, experiments were carried out at four temperatures (*viz*. 303, 313, 323 and 333 K) using a temperature controlled water bath (Make: International Commercial Traders, Model: B/CH). Similar procedure was followed for mechanically stirred system, in which a hot metal plate stirrer was used. A schematic of the experimental setup used in the experiments is given in supplementary material (Fig. S.1a and b).

2.3 Experimental protocols: Toluene (20 mL) with an initial DBT concentration of 100 ppm has been used as model fuel. The oxidant system employed for oxidative desulfurization was H_2O_2 promoted by formic acid, which formed performic acid (PFA), HCOOOH, *in–situ* in the reaction system. The experiments were planned in three categories, which have been depicted in Table 1. The exact composition of the reaction mixture in each experimental protocol is given in Table S.1 in the supplementary material. Composition of reaction mixture was decided on the basis of preliminary experiments, which have been described in supplementary material provided with the manuscript (Figs. S.2 and S.3). TBAB was used as phase transfer agent

(PTA). The amount of PTA added to reaction mixture was varied in the range of 0.25 – 0.1 g. In some experiments, the static pressure on the reaction solution was raised to 1.6 bar using a nitrogen cylinder with two–stage regulator. During the reaction, aliquots of reaction mixture (0.5 mL) were withdrawn every 15 min and were analyzed for the residual DBT concentration. All experiments were done in triplicate to assess reproducibility of results.

2.4 Analysis: The residual concentration of DBT in the aliquots of reaction mixture was analyzed using Shimadzu High Performance Liquid Chromatography (HPLC, Model: SPD–20A) equipped with a reverse phase C–18 column (5 μm, 4.6 mm × 250 mm) and UV detector at 287 nm. The mobile phase was a mixture of acetonitrile and water (80:20 v/v). The formation of sulfone in oxidative desulfurization was confirmed using FTIR analysis after completion of reaction. To identify the intermediates during DBT oxidation, GC–MS analysis of the same reaction sample was performed using Varian 240– GC equipped with VF–5ms column (30 m × 0.25 m ID, DF = 0.25). The temperature program was as follows: injection temperature = 250^{o}C, column temperature = 100^{o}C at zero time and increased to 300^{o}C at a ramping rate of 7^{o}C/min.

2.5 Characterization of oxidized product

HPLC chromatograph: Representative HPLC chromatographs of the aliquots of reaction mixture are shown in Fig. 1. Peaks corresponding to DBT and DBT sulfone were obtained at retention times of 9.1 and 3.9 min, respectively.

FTIR analysis: Fig. 2 compares the IR spectra of reaction mixture before and after DBT oxidation reaction. Fig. 2 shows two different characteristic peaks of sulfone compound at 1370 cm^{-1} and 1035 cm^{-1}, while characteristic peak at 917 cm^{-1} represents the sulfoxide compound confirming the oxidation of DBT during treatment.

GC–MS analysis*:* The high resolution GC–MS total ion chromatograms of reaction mixture (initial and after completion of the reaction) are shown in Figs. 3.A and 3.B, respectively. The molecular mass of DBT was determined to be 184.3, which is close to the calculated value of 184.26. The oxidized products were found to have a mass of 199.6 and 216.03 giving a mass

difference of 16 and 32 units with respect to DBT, respectively. These additional units correspond to the mass of 1 and 2 oxygen atoms. The peaks obtained at 20.08, 22.1 and 25.3 min correspond to DBT, DBT sulfoxide and DBT sulfone, respectively. The major ions obtained at different m/z (% intensity, proposed derivation from molecular ion, M) values are 200 (10, [M]+), 184 (100, [M–O]+), 171 (12.5, [M–CHO]+), 139 (20, [M–COH–S]+), 216 (100, [M]+), 187 (37.5, [M–COH]+), 168 (23, [M–O–S]+), 160 (10, [M–CO–CO]+), and 150 (7.5, [M–OH–OH–S]+). The mass spectra of DBT, DBT sulfone and DBT sulfoxide are shown in Figs. 4.A – 4.C.

3. Mathematical Models

In the analysis of the physical mechanism of PTA–assisted ultrasonic oxidative desulfurization, we have used two models, *viz*. kinetic model for PTA–assisted oxidative desulfurization system and model for cavitation bubble dynamics, as described below:

3.1 Kinetic model for PTA–assisted oxidative desulfurization

In the classic review on science and engineering of phase transfer catalysis, Naik and Doraiswamy[19] have described the general considerations in modeling of PTA assisted reactions. PTA enhances slow (or kinetically controlled) reactions as well as fast reactions, which occur – either partially or completely – in diffusion film at the interphase. Therefore, Naik and Doraiswamy[19] have recommended that a model for PTA–assisted reaction must consider all individual steps in the PTA cycle, *i.e*. interphase mass transfer, ion exchange and the organic phase reactions. The active catalyst concentration (or the concentration of the PTA–anion complex) in the organic phase is an important parameter. However, the concentration of PTA–anion complex in organic phase remains constant in presence of large excess of nucleophilic reagent (performic acid in the context of present study). Enhanced mass transfer rate in presence of ultrasound also contributes to achieving constant concentration of PTA–anion complex in organic phase. The ion exchange rate has also been revealed to be much faster (~ 10×) than the

rate of reaction in organic phase.[20] Under these circumstances, the organic reaction is the rate controlling step, and is usually modeled using pseudo–1st order kinetics. Several studies on modeling of phase transfer catalyzed liquid–liquid heterogeneous reaction have confirmed suitability of pseudo–1st order kinetics for the overall reaction.[21,22] Bhattacharya[23] has presented a general kinetic model for liquid–liquid phase transfer catalyzed reactions, in which he has pointed out that assumption of constant concentration of PTA–anion complex is valid only when the rate of transfer of nucleophile to organic phase equals its consumption through organic reaction.

As stated earlier, we have determined the kinetic constants of PTA–assisted oxidative desulfurization in different experimental protocols using the model proposed by Zhao et al.[16] This model is based on the model of Maw–Ling and Chen[24] for PTA–assisted synthesis of formaldehyde acetals from alcohols and dibromomethane in an alkaline solution of KOH and organic solvent. This model has been developed for mechanically agitated system. We have used this model for ultrasonic desulfurization in view of the predominant influence of micro–convection generated by ultrasound on the reaction system. Zhao et al.[16] have also proposed that complexation of the anion of oxidant ($HCOOO^-$) with cation of the PTA reduces its polarity, which enable faster transport to the organic phase. Although this hypothesis is perceivable, it should be noted that the PTA–anion still has ionic character– as the net charge is not neutralized after complexation. For the convenience of the reader, we have reproduced below this model.

The oxidant in present study, *viz*. performic acid, forms by reaction between formic acid and H_2O_2 as follows:

$$HCOOH + H_2O_2 \longrightarrow HCOOOH + H_2O$$

Performic acid undergoes dissociation to yield nucleophilic anionic oxidant species $HCOOO^-$ as follows:

$$HCOOOH \rightleftharpoons HCOOO^- + H^+$$

The nucleophile anion $HCOOO^-$ forms a complex with cation of PTA (quaternary ammonium salt), represented as Q^+Br^- as:

$$HCOOO^- + Q^+Br^- \longrightarrow [HCOOO--Q--Br] \quad (1)$$

Desulfurization reaction occurs in the organic phase in two steps: (1) formation of PTA–oxidant complex in the aqueous phase (represented by subscript *aq*), and (2) transfer of the complex across interphase to organic phase (represented by subscript *org*). This process is reversible and is characterized by two rate constants (k_1 and k_{-1}, for forward and backward reactions, respectively). Usually, the intrinsic reaction between PTA and the oxidant is very fast. Hence, the overall rate constants k_1 and k_{-1} are essentially functions of interphase mass transfer rate (which can be called as rate limiting step). In a liquid–liquid heterogeneous system, the rate of mass transfer across interphase is a function of the interfacial area. The second step (reaction 3) is the irreversible oxidation of sulfur compound in the organic phase and this is characterized by rate constant k_2.

$$(Q^+Br^-)_{aq} + (HCOOO^-)_{aq} \underset{k_{-1}}{\overset{k_1}{\rightleftharpoons}} (Br^-)_{aq} + (Q^+CHOOO^-)_{org} \quad (2)$$

$$(Q^+CHOOO^-)_{org} + (C_{12}H_8S)_{org} \xrightarrow{k_2} (C_{12}H_8SO)_{org} + (Q^+)_{org} + (HCOO^-)_{org} \quad (3)$$

The rate of oxidation of DBT in organic phase (or formation of product DBT sulfone $[C_{12}H_8SO]_{org}$) is written as:

$$\frac{d[C_{12}H_8SO]_{org}}{dt} = k_2[Q^+HCOOO^-]_{org}[C_{12}H_8S]_{org} \quad (4)$$

In order to determine the rate of reaction in organic phase, we need to know the concentration of PTA–anion complex in organic phase. The formation of PTA–oxidant complex $(Q^+HCOOO^-)_{org}$ can be described by following rate expression as per equations 2 and 3 given above:

$$\frac{d[Q^+HCOOO^-]_{org}}{dt} = k_1[Q^+Br^-]_{org}[HCOOO^-]_{aq} - k_{-1}[Q^+HCOOO^-]_{org}[Br^-]_{aq} - k_2[Q^+HCOOO^-]_{org}[C_{12}H_8S]_{org} \quad (5)$$

At steady–state, the net concentration of the PTA–oxidant complex in the organic phase stays

constant and this gives the condition: $\frac{d[Q^+HCOOO^-]_{org}}{dt} = 0$ (6)

Other factors that also contribute to constant concentration of PTA–oxidant complex in organic phase are fast ion exchange and mass transfer across interphase, and large excess of the oxidant and PTA, as compared to the concentration of sulfur compound in organic phase.[19] It follows therefore that:

$$k_1[Q^+Br^-]_{org}[HCOOO^-]_{aq} = k_{-1}[Q^+HCOOO^-]_{org}[Br^-]_{aq} + k_2[Q^+HCOOO^-]_{org}[C_{12}H_8S]_{org} \quad (7)$$

The PTA exists in the organic phase of the reaction system in pure form Q^+Br^- as well as in the form of the complex. Hence, the total concentration of PTA cation $[Q^+]_{org}$, which forms complex with nucleophilic oxidant is written as:

$$\left[Q^+\right]_{org} = [Q^+Br^-]_{aq} + [Q^+HCOOO^-]_{org} \quad (8)$$

Substituting for $[Q^+Br^-]_{aq}$ as $[Q^+]_{org} - [Q^+HCOOO^-]_{org}$ in equation 7, we get:

$$[Q^+HCOOO^-]_{org} = \frac{k_1[Q^+]_{org}[HCOOO^-]_{aq}}{k_1[HCOOO^-]_{aq} + k_{-1}[Br^-]_{aq} + k_2[C_{12}H_8S]_{org}} \quad (9)$$

Now substituting eqn. (9) in eqn. (4), the rate of reaction of DBT oxidation in organic phase is:

$$\frac{d[C_{12}H_8SO]_{org}}{dt} = \frac{k_1k_2[Q^+]_{org}[HCOOO^-]_{aq}[C_{12}H_8S]_{org}}{k_1[HCOOO^-]_{aq} + k_{-1}[Br^-]_{aq} + k_2[C_{12}H_8S]_{org}} \quad (10)$$

Due to convection present in the system (either in the form of mechanical agitation or ultrasound irradiation), the rate of interphase mass transfer of $(HCOOO^-)_{aq}$ can be assumed to be very fast. This results in rapid accumulation of $(HCOOO^-)_{aq}$ and $(Q^+)_{org}$ in the organic phase. This favors the forward reaction of eq. (2). Moreover, the intrinsic kinetics of the DBT oxidation reaction in the organic phase is also likely to be much slower than the dissociation of performic acid. Under these conditions, the following inequality holds true:

$$k_1[HCOOO^-]_{aq} >> k_{-1}[Br^-]_{aq} + k_2[C_{12}H_8S]_{org} \quad (11)$$

With this, the rate expression for product formation gets transformed as:

$$\frac{d[C_{12}H_8SO]_{org}}{dt} = k_2[Q^+]_{org}[C_{12}H_8S]_{org} \quad (12)$$

The stoichiometry of reaction between DBT (reactant) and DBT–sulfone (product) is essentially one. Hence, one can easily substitute rate of formation of product in terms of rate of disappearance of reactant (DBT):

$$-\frac{d[C_{12}H_8S]_{org}}{dt} = \frac{d[C_{12}H_8SO]_{org}}{dt} \quad (13)$$

Therefore, equation 12 becomes:

$$\frac{d[C_{12}H_8S]_{org}}{dt} = -k_2[Q^+]_{org}[C_{12}H_8S]_{org} \quad (14)$$

Since the PTA concentration is usually in large excess, and that mass transfer rate across interphase is also fast, its total concentration of quaternary cation (in free and complex form) in organic phase stays constant. Hence, we can club together the rate constant k_2 and the concentration of PTC, $[Q^+]_{org}$ to give a new constant, k_3.

$$\frac{d[C_{12}H_8S]_{org}}{dt} = -k_3[C_{12}H_8S]_{org}, \text{ where } k_3 = k_2[Q^+]_{org} \quad (15)$$

Integrating the above equation between limits, at $t = 0$, $[C_{12}H_8S]_{org} = [C_{12}H_8S]_{org,0}$, and at $t = t$, $[C_{12}H_8S]_{org} = [C_{12}H_8S]_{org,t}$, we get:

$$\ln\frac{[C_{12}H_8S]_{org,0}}{[C_{12}H_8S]_{org,t}} = kt \quad (16)$$

where, k is overall or gross pseudo–1st order rate constant for oxidative desulfurization process. Thus, analysis of Zhao et al.[16] essentially proves that with excess of oxidant as well as PTA employed during oxidative desulfurization (as is the case in present study), the overall oxidative desulfurization reaction follows pseudo–1st order kinetics.

3.2 Simulations of cavitation bubble dynamics

In the present case, the reaction system is a two–phase mixture, *viz*. organic phase (toluene) and aqueous phase (performic acid). Passage of ultrasound through the reaction

mixture induces micro–streaming (*i.e.* oscillatory motion of fluid elements) in both phases, but due to larger volume fraction in reaction mixture, the micro–streaming in toluene contributes mostly to the emulsification of organic and aqueous phases. The micro–streaming velocity is calculated as: $u = P_A/\rho_L c$. The acoustic pressure amplitude (P_A) in the medium was determined as 150 kPa using calorimetric measurements. For toluene, ρ_L (density) = 867 kg/m^3 and c (sonic velocity) = 1275 m/s, and thus, u = 0.137 m/s.

The magnitudes of physical and chemical effects of cavitation bubbles have been determined using diffusion limited ordinary differential equation model proposed by Toegel et al.[25] It should be noted that cavitation phenomena occurs in both organic medium (toluene) and aqueous medium (performic acid). However, since the DBT oxidation reaction occurs in organic phase, we have considered the cavitation bubble dynamics phenomena in toluene only in our model. Cavitation phenomenon occurring in aqueous medium mainly contributes to emulsification of the two phases, due to the convection induced by radial motion of transient cavitation bubbles. The diffusion limited model of Toegel et al.[25] is based on the comprehensive partial differential equation model of Storey and Szeri[26] who showed that solvent vapor transport and entrapment in the cavitation bubble, leading to formation of radicals, is essentially a diffusion limited process. This model has been extensively described in previous papers.[27–29] For convenience of the readers, the essential equations and thermodynamic data of this model have been provided in the supplementary material (Tables S.2 and S.3). The model is essentially a set of 4 ordinary differential equations: (1) Keller–Miksis[30] equation for the radial motion of the bubble, (2) equation for the diffusive flux of water vapor and heat conduction through bubble wall, and (3) overall energy balance. Thermal conductivity of the bubble contents and diffusion coefficient of water vapor inside the bubble are determined using Chapman–Enskog theory using Lennard–Jones 12–6 potential. An air bubble has been considered for simulations. The condition for bubble collapse is taken as the first compression after an initial expansion. Various parameters used in the simulation of bubble dynamics equation and their numerical values are as follows:

Ultrasound frequency (f) = 35 kHz; Ultrasound (or acoustic) pressure amplitude (P_A) = 150 kPa; Equilibrium bubble radius (R_o) = 5 μm; Vapor pressure of toluene was calculated using Antoine type correlation at the temperature of the reaction (298 K). Various physical properties of toluene are as follows: density (ρ_L) = 867 kg/m^3, kinematic viscosity (ν) = 6.8 × 10^{-7} Pa–s, surface tension (σ) = 0.0285 N/m, and sonic speed (c) = 1275 m/s, static pressure (P_o) = 101.3 kPa (for experiments at atmospheric static pressure) or 162 kPa (for experiments with elevated static pressure).

3.3 Estimation of physical and chemical effects of cavitation

The chemical effect of cavitation bubble dynamics (or the sonochemical effect) is generation of small chemical species (including some radical species) from thermal dissociation of gas and solvent vapor molecules entrapped in the bubble at the moment of transient collapse – when the temperature and pressure conditions in the bubble reach extreme. Numerical solution of the diffusion–limited cavitation bubble dynamics model gives the number of solvent (toluene) vapor molecules present in the bubble at the point of minimum radius during radial motion along with the temperature and pressure peak reached in the bubble. Due to extreme temperature and pressure in the bubble, and also very high concentrations of chemical species due to extremely small volume of the bubble, the rates of different chemical reactions occurring in the bubble are extremely fast, and thermal equilibrium is likely to prevail all through the radial motion of the bubble.[31] In view of this hypothesis of Brenner et al.,[31] the equilibrium mole fraction of various species in the bubble (at the conditions of temperature and pressure at first the compression of the bubble) resulting from thermal dissociation of air (oxygen and nitrogen) and toluene molecules have been calculated using Gibbs free–energy minimization technique.[32]

The principal physical effect of cavitation is generation of strong micro–convection in the bulk medium through two phenomena, *viz*. micro–turbulence, and shock or acoustic waves. The magnitudes of these two parameters can be calculated using bubble dynamics model as follows:[33–35]

Velocity of micro–turbulence: $V_{\text{turb}} = \frac{R^2}{r^2}\left(\frac{dR}{dt}\right)$ (17)

Pressure amplitude of shock waves: $P_{AW} = \rho_L \frac{R}{r}\left[2\left(\frac{dR}{dt}\right)^2 + R\frac{d^2R}{dt^2}\right]$ (18)

r is the distance from bubble center. A representative value of r is taken as 1 mm.

3.4 Arrhenius (kinetic) and thermodynamic analysis

Arrhenius analysis was done using pseudo–1st order kinetic constants (at various temperatures) obtained from the model of Zhao et al.[16] in different experimental categories. The activation energy (E_a) and frequency factor (A) of desulfurization in different experimental categories were estimated using plots of ln k vs $1/T$. The basic thermodynamic properties of the reaction system could be determined using Eyring equation as follows:

$$\ln\frac{k}{T} = -\frac{\Delta H}{R}\frac{1}{T} + \ln\frac{k_b}{h} + \frac{\Delta S}{R} \quad (19)$$

$$\Delta H = E_a - RT \quad (20)$$

$$\Delta G = \Delta H - T\Delta S \quad (21)$$

k_b and h are Boltzmann and Planck's constants, respectively. The results of Arrhenius analysis can be used to determine the thermodynamic parameters of ΔH, ΔS and ΔG.

4. Result and Discussion

4.1 Trends in DBT oxidation

The time histories of DBT oxidation in different experimental categories are depicted in Figs. 5.A and B. Results of DBT oxidation in different experimental categories are summarized in Table 1. As stated earlier, the DBT oxidation was carried out at 4 temperatures. However, the temperature at which the highest DBT oxidation (with highest kinetic constant) was different for mechanical stirred and ultrasound-assisted systems. For mechanically stirred system, the highest DBT oxidation was obtained at 333 K, while for ultrasound-assisted systems, the temperature

for the highest DBT oxidation was 313 K. The results depicted in Table 1 and Figs. 5A& B correspond to these temperatures. The trends in DBT oxidation in different experimental categories reveal following distinct features:

(1) Comparing the extent of DBT oxidation for categories A.2 and B.2, 3.1× (or 3.1–fold) rise in oxidation is seen when PTA is used in presence of ultrasound. On the other hand, comparing the results for categories A.1 and B.1, relatively lesser rise of 2.25× (or 2.25–fold) in oxidation is seen for PTA applied in mechanically stirred systems. Thus, the enhancement in DBT oxidation in presence of PTA is more pronounced for ultrasonic systems than mechanically stirred systems. This result is in complete concurrence with conclusion of Hagenson et al.[11] that enhancement effect of PTA on reaction kinetics acquires higher significance in presence of ultrasound.

(2) Comparison of results of categories B.1 and B.2 reveals that effect of PTA is more pronounced for ultrasound–assisted system than mechanically agitated one. This is yet another proof of the synergism between mechanism of ultrasound and PTA – which is corroborated by conclusions of Hagenson et al.[11]

(3) Reduction in DBT oxidation at elevated static pressure, as evident from comparison of the results of the categories B.2 and C.1, is attributed to suppression of the transient cavitation phenomenon at elevated static pressure, as explained in greater detail subsequently.

4.2 Arrhenius and thermodynamic analysis

The kinetic analysis of the DBT oxidation reactions at different temperatures (*viz*. 303, 313, 323, and 333 K) in various experimental categories using pseudo–1st order model (eq. 16) is presented in Figs. S.4.A.1–D.1 in supplementary material. The corresponding Arrhenius plots are shown in Figs. S.4.A.2–D.2 in supplementary material. Arrhenius and thermodynamic parameters of the oxidative desulfurization in different experimental categories are summarized in Table 2.A and B, respectively. The characteristic variations in Arrhenius parameters evident from results presented in Table 2.A are as follows:

(1) Use of PTA in mechanically stirred system reduces the activation energy of oxidative desulfurization, as observed from comparison of the activation energies in categories A.1 and B.1. This result is in concurrence with observations of Zhao et al.[16]

(2) The ultrasound–assisted systems (categories A.2 and B.2) have significantly lower activation energies as compared to mechanically stirred systems (categories A.1 and B.1, respectively). Moreover, it is interesting to note that the use of PTA in ultrasound assisted desulfurization systems leads to increase in activation energy, as seen from the Arrhenius parameters for categories A.2 and B.2.

(3) The frequency factors for ultrasound assisted systems (categories A.2 and B.2) are one to two orders of magnitude smaller than the mechanically stirred system (categories A.1 and B.1). Use of PTA with ultrasound leads to rise in frequency factor, as evident from comparison of frequency factors for categories A.2 and B.2.

(4) Scatter of data points in Arrhenius plots and low regression coefficients in Figs. S.4.B.2 and 4.D.2 (corresponding to the systems with ultrasound) are attributed to the inverse effect of temperature on intensity of transient cavitation. Both physical and chemical effects of cavitation diminish with increasing temperature. The reason underlying this effect is large evaporation of solvent vapor (due to high vapor pressure) and subsequent entrapment in the bubble at elevated temperature. The entrapped vapor "cushions" the transient collapse of the cavitation bubble. This causes reduction in the intensity of collapse (the peak temperature and pressure reached in the bubble) and also the physical/chemical effects associated with it. Consequently, the rate of reactions that are accelerated by physical/chemical effects of cavitation also reduce with temperature. This phenomenon violates the postulate of increase in rate of reaction with temperature in Arrhenius theory. Therefore, kinetic data of ultrasound–assisted reactions (in the present context experimental categories A.2 and B.2) shows a scatter when fitted to the Arrhenius model leading to low regression coefficients as seen in Figs. S.4.B.2 and S.4.D.2 in supplementary material. However, despite this limitation, the trends in the Arrhenius parameters

obtained for different experimental categories reveal a physically meaningful picture of the mechanism of PTA–assisted ultrasonic oxidative desulfurization.

The trends in thermodynamic parameters that can be identified from the results presented in Table 2.B are as follows: (1) Use of PTA in mechanically stirred system leads to reduction in ΔH and ΔG and increase in $-\Delta S$. (2) Use of PTA in ultrasound assisted system shows rather opposite trend that ΔH increases, while $-\Delta S$ and ΔG reduce in presence of PTA. (3) As compared to mechanically stirred systems, ΔH and ΔG values for ultrasound–assisted systems are significantly smaller, while $-\Delta S$ values are higher.

4.3 Results of cavitation bubble dynamics simulations

The summary of results of cavitation bubble dynamics simulations for a 5 micron air bubble in toluene are presented in Table 3. Representative graphical simulations of the radial motion of cavitation bubble are shown in Figs. S.5 and S.6 in supplementary material. It could be seen that the temperature and pressure conditions in the cavitation bubble reach extreme during transient collapse at atmospheric static pressure, which are sufficient to cause thermal dissociation of N_2, O_2 and toluene (C_6H_5–CH_3) molecules entrapped in the bubble into numerous chemical species – some of which are radical species. The predominant species generated during transient cavitation, which can contribute to DBT oxidation, is the $O^{\bullet}$ radical. Shock waves with high pressure amplitude emitted by cavitation bubble can create very fine emulsion of aqueous/organic phases with enormous interfacial area, which can boost the reaction kinetics.

Raising of the static pressure in reaction mixture results in drastic reduction of physical and chemical effects of transient cavitation. Not only the temperature and pressure peaks generated at transient bubble collapse drop sharply, but the magnitudes of shock waves (or acoustic pressure waves) and micro–turbulence generated by the bubble also shows marked reduction. Moreover, no formation of any radical species is seen from thermal dissociation of the bubble contents at the moments of transient collapse at elevated static pressure.

4.4 Discussion

Concurrent analysis of the DBT oxidation in different experimental categories, simulations of cavitation bubble dynamics, and the trends in Arrhenius and thermodynamic parameters give an interesting mechanistic account of the PTA–assisted oxidative desulfurization as described below:

(1) Mechanical agitation of reaction mixture at 300 rpm generates limited interfacial area, which results in low (~ 28.3%) DBT oxidation. PTA cation forms a complex with oxidant anion, which is transported across the interphase. After completion of the oxidation reaction in organic phase, the PTA–cation returns to the aqueous phase. The chemical mechanism of PTA–assisted oxidative desulfurization with mechanical agitation is depicted in scheme S.1 given in supplementary material. It could be perceived from scheme S.1 that the process has purely ionic character. Addition of PTA to this system enhances DBT oxidation by more than 2× as a result of faster and effective transfer of oxidant across interface. This is reflected in reduction of activation energy of the oxidative desulfurization, as pointed out by Zhao et al.[16] For same reason, the net enthalpy change (ΔH) for oxidative desulfurization also reduces with use of PTA.

(2) Despite very low activation energy and intense emulsification, the extent of DBT oxidation in ultrasound assisted system (category A.2) is almost same as that for mechanically agitated system (category A.1). This result is attributed to radical based mechanism of ultrasound–assisted oxidative desulfurization (as shown in scheme S.2 given in supplementary material). The oxidative radicals ($O^{\bullet}$) generated by transient bubble collapse are highly unstable and do not diffuse or penetrate much in the reaction medium from the point of bubble collapse. Hence, the probability of their interaction with DBT molecules is rather limited, which is reflected in low value of frequency factor (A) as compared to the mechanical agitated system (category A.1), and low DBT oxidation. Nonetheless, since $O^{\bullet}$ radicals are extremely energetic species (oxidation potential of 2.42 eV), the activation energy for the DBT oxidation induced by these species is quite small. For the same reasons, ΔH for category A.2 is much smaller than that for

category A.1.

(3) With simultaneous use of PTA and ultrasound (as in categories B.2 and C.1), the chemical mechanism of the oxidative desulfurization has dual character, *viz*. ionic and radical. The cation of PTA forms a complex with anion of oxidant. This reduces the polarity of the oxidant anion, which assists its effective transfer across interface to non–polar organic phase. It should however be noted that complexation of oxidant–anion with PTA–cation does neutralize latter's polarity, and hence, the overall mechanism of oxidative desulfurization has still ionic character. On a comparative basis, the process of complex formation between PTA–cation and oxidant–anion, the transfer of this complex across interface and the reaction between oxidant and DBT molecules, requires higher activation energy than the radical–induced DBT oxidation within organic phase. However, as the amount of oxidant and PTA present in the system is in large excess as compared to DBT (more specifically 1.24 mM of PTA, 25 mM of PFA oxidant, and 0.54 mM of DBT), the contribution of PTA–based oxidation to overall DBT oxidation is much higher than radical–induced oxidation. Thus, the chemical mechanism of PTA–assisted ultrasonic oxidative desulfurization is predominantly ionic, which is manifested in terms of higher activation energy as compared to ultrasonic oxidative desulfurization. Explanation for ~ 4× higher ΔH value for category B.2 as compared to category A.2 can also be given along similar lines. Due to contribution of radical–induced reactions to overall DBT oxidation in category B.2, the activation energy for this category is ~ 2× lesser than that for category B.1, in which PTA is applied with mechanical stirring. The role of ultrasound and cavitation in experimental categories B.2 and C.1 is more or less of physical nature, *i.e*. emulsification between organic and aqueous phase.

(4) Reduction in intensity of transient cavitation at elevated static pressure in category C.1, as indicated by results of simulation of cavitation bubble dynamics, is manifested in terms of lesser emulsification and interfacial area, as compared to the category B.2. The physical and chemical effects of transient cavitation are practically eliminated at elevated static pressure. This causes

significant reduction in intensity of micro–convection in the reaction system, which in turn, adversely affects emulsification and interfacial area. In this case, the ultrasonic system resembles a mechanical stirred system (as in category B.1). This essentially results in lesser DBT oxidation in category C.1. However, the micro–streaming induced by ultrasound (which remains unaffected by elevated static pressure) generates finer emulsion between phases, as compared to (macroscopic) mechanical stirring. Addition of PTA to the reaction system further boosts the extent of DBT oxidation. The beneficial effect of these two factors is manifested in significantly higher (> 2×) DBT oxidation, as compared to categories A.1 and A.2.

(5) The entropy change values ($-\Delta S$) in different experimental categories are again manifestations of the predominant chemical mechanism of oxidative desulfurization. The highest ($-\Delta S$) values are seen for category A.2, in which the chemical mechanism for oxidative desulfurization is purely radical–based and reactions occur almost instantly. The ($-\Delta S$) values for mechanically stirred system increase with addition of PTA, indicating faster reactions. ($-\Delta S$) values for category B.2 are intermediate between that of categories B.1 and A.2, indicating dual (ionic and radical induced) nature of the chemical mechanism of the PTA–assisted oxidative desulfurization. The dual nature of chemical mechanism in category B.2 also results in pseudo–1st order kinetic constants of intermediate value between the constants for categories A.2 and B.1.

(6) Despite significantly dissimilar chemical mechanisms that lead to dissimilar values of ΔH and ($-\Delta S$), the Gibbs energy change (ΔG) is almost similar (±5%) for experimental categories B.1 and B.2, in which PTA was simultaneously applied with ultrasound. This essentially is an indication of the physical role played by ultrasound in PTA–assisted oxidative desulfurization. Moreover, lesser (ΔG) values for categories B.1 and B.2, as compared to categories A.1 and A.2, respectively, point out supportive effect of the PTA in enhancement of the oxidative desulfurization by effective interphase transport of oxidant anion.

5. Conclusion

Concurrent analysis of extent of DBT oxidation and Arrhenius & thermodynamic parameters for different experimental conditions, and results of simulations of cavitation bubble dynamics presented in this study has revealed a cogent and coherent picture of the physical mechanism of the PTA–assisted ultrasonic oxidative desulfurization process. Essentially, this study has identified and established the links (or interactions) between the individual mechanisms of PTA and ultrasound/ cavitation in oxidative desulfurization process. Although ultrasonic oxidative desulfurization has the lowest activation energy and enthalpy change with the highest negative entropy change, the overall DBT oxidation achieved in this process is lesser due to low frequency factor, which is a consequence of high instability of the radicals generated by transient cavitation. Thus, contribution of chemical effect of transient cavitation to DBT oxidation is relatively small. The predominant mechanism of PTA–assisted oxidative desulfurization is ionic, which results in relatively higher activation energy and enthalpy change as compared to ultrasonic oxidative desulfurization. The synergistic effect of fine emulsification generated due to physical effect of micro–convection induced by transient cavitation and ultrasound, and PTA–assisted effective interphase transport of oxidant leads to almost complete conversion of DBT to DBT sulfone. It is thus established that prevalent role of ultrasound and cavitation in PTA–assisted ultrasonic oxidative desulfurization process is of physical nature that helps in boosting the beneficial effect of PTA for enhancement of DBT oxidation.

Acknowledgment

Authors would like to thank Mr. Pritam Kumar Dikshit for his help in manuscript preparation.

Supplementary Material

The following supplementary materials have been provided with this manuscript: (1) schematic diagram of the experimental setup, (2) preliminary experiments for determination of composition of reaction mixture, (3) Model equations and thermodynamic data for cavitation

bubble dynamics, (4) Experimental categories with exact composition of reaction mixture, (5) Kinetic analysis of oxidative desulfurization under ultrasound treatment and mechanical stirring using performic acid as oxidant coupled with TBAB as phase transfer agent, (6) Simulations of radial motion of a 5 micron air bubble in toluene at elevated static pressure, (7) Simulations of radial motion of a 5 micron air bubble in toluene at atmospheric static pressure, (8) Reaction mechanism for only ultrasound assisted oxidative desulfurization and PTA–assisted ultrasonic oxidative desulfurization.

References

1. V. C. Srivastava, *RSC Adv*., 2012, **2**, 759–783.
2. C. Song, U. T. Turaga and X. Ma, 2006, DOI: 10.1081/E–ECHP–120007732, 651–661.
3. V. S. Moholkar, V. A. Nierstrasz and M. M. G. C. Warmoeskerken, *Autex Res. J.* 2003; **3**, 129–138.
4. M. M. G. C. Warmoeskerken, P. van der Vlist, V. S. Moholkar, V. A. Nierstrasz, *Colloids Surf. A* 2002, **210**, 277–285.
5. S. Chakma, V. S. Moholkar, *Chem. Eng. J.* 2011, **175**, 356–367.
6. H. A. Choudhury, R. S. Malani, V. S. Moholkar, *Chem. Eng. J.* 2013, **231**, 262–272.
3. L. K. Doraiswamy, Oxford University Press*,* New York, 2001.
4. H. Mei, B. W. Mei and T. F. Yen, *Fuel*, 2003, **82**, 405–414.
5. O. Etemadi and T. F. Yen, *Energ. Fuel,* 2007, **21**, 2250–2257.
6. M. W. Wan and T. F. Yen, *Appl. Catal. A*., 2007, **319**, 237–245.
7. L. C. Hagenson and L. K. Doraiswamy, *Chem. Eng. Sci.,* 1994, **49**, 4787 – 4800.
8. L. C. Hagenson and L.K. Doraiswamy, *Chem. Eng. Sci.,* 1998, **53**, 131–148.
9. M. K. Bolla, H. A. Choudhury and V. S. Moholkar, *Ind. Eng. Chem. Res.,* 2012, **51**, 9705–9712.
10. J. B. Bhasarkar, S. Chakma and V. S. Moholkar, *Ind. Eng. Chem. Res.,* 2013, **52**, 9038–9047.
11. J. B. Bhasarkar, S. Chakma and V. S. Moholkar, *Ultrason. Sonochem.,* 2015, **24**, 98–

106.

12. D. Zhao, H. Ren, J. Wang, Y. Yang and Y. Zhao, *Energ. Fuel,* 2007, **21**, 2543–2547.

13. S. Chakma and V. S. Moholkar, *Ind. Eng. Chem. Res.,* 2014, **53**, 6855–6865.

14. P. R. Gogate, P. A. Tatake, P. M. Kanthale and A. B. Pandit, *AIChE J.,* 2002, **48**, 1542–1560.

15. S. D. Naik and L. K. Doraiswamy, *AIChE J.,* 1998, **44**, 612–646.

16. M–L. Wang and H–M. Yang, *Ind. Eng. Chem. Res.,* 1990, **29**, 522–526.

17. M–L. Wang and H–M. Yang, *Ind. Eng. Chem. Res.,* 1991, **30**, 631–635.

18. M–L. Wang and H–M. Yang, *Chem. Eng. Sci.,* 1991, **46**, 619–627.

19. A. Bhattacharya, *Ind. Eng. Chem. Res.,*1996, **35**, 645–652.

20. M–L. Wang and W–H. Chen, *Ind. Eng. Chem. Res.,* 2009, **48**, 1376–1383.

21. R. Toegel, B. Gompf, R. Pecha and D. Lohse, *Phys. Rev. Lett.*, 2000, **85**, 3165–3168.

22. B. D. Storey and A. J. Szeri, *Proc. R. Soc. London, Ser. A*, 2000, **456**, 1685–1709.

23. T. Sivasankar, A. W. Paunikar and V. S. Moholkar, *AIChE J*., 2007, **53**, 1132–1143.

24. V. S. Moholkar, S. P. Sable and A. B. Pandit, *AIChE J*., 2000, **46**, 684–694.

25. S. J. Krishnan, P. Dwivedi and V. S. Moholkar, *Ind. Eng. Chem. Res*., 2006, **45**, 1493–1504.

26. J. B. Keller and M. J. Miksis, *J. Acoust. Soc. Am.,* 1980, **68**, 628–633.

27. M. Brenner, S. Hilgenfeldt and D. Lohse, *Rev. Mod. Phys.,* 2002, **74**, 425–484.

28. Chemical Equilibrium Calculation, http://navier.engr.colostate.edu/~dandy/code/code–4/index.html, (accessed January 2013).

29. T. G. Leighton, Academic Press, San Diego, 1994.

30. S. Grossmann, S. Hilgenfeldt, M. Zomack and D. Lohse, *J. Acoust. Soc. Am.,* 1997, **102**, 1223–1227.

31. V. S. Moholkar and M. M. C. G Warmoeskerken, *AIChE J.,* 2003, **49**, 2918–2932.

Table 1: Summary of DBT oxidation in four experimental categories

Experimental Category	Solvent: Toluene		
	η%[#]	***k*** **(min^{-1})**[*]	***R*^{2}**
A1. MS +PFA	28.30 ± 1.12	4.13×10^{-3}	0.97
A2. US + PFA	31.22 ± 0.98	4.43×10^{-3}	0.95
B1. MS +PFA + TBAB	63.50 ± 0.92	1.22×10^{-2}	0.96
B2. US +PFA + TBAB	96.65 ± 1.06	4.26×10^{-2}	0.97
C.1 US + PFA+ TBAB + ESP (1.8 bar)	77.63 ± 1.39	1.52×10^{-2}	0.85

* – pseudo–1st order kinetic constant, *k*, obtained at reaction temperature of 313 K for ultrasound assisted desulfurization experiments, and 333 K for experiments using mechanical stirring. *Abbreviations:* MS – mechanical stirring, US – ultrasound-assisted treatment (or under sonication), ESP – elevated static pressure. # – percentage DBT oxidation (η) calculated as: $\left[\left(\textbf{initial DBT concn.} - \textbf{final DBT concn.}\right)/\textbf{initial DBT concn.}\right] \times 100$

Table 2: Arrhenius and thermodynamic analysis of PTA–assisted oxidative desulfurization

Experimental Category	Parameter	Temperature (K)				E_a (kJ/mol)	A (mol/L min)
		303	313	323	333		
A. Kinetic and Arrhenius analysis							
MS + PFA	k (min^{-1})	1.12×10^{-3}	2.63×10^{-3}	3.42×10^{-3}	4.20×10^{-3}	38.74	5805.14
	R^2	0.92	0.97	0.94	0.95		
US + PFA	k (min^{-1})	4.40×10^{-3}	6.10×10^{-3}	5.80×10^{-3}	5.59×10^{-3}	5.96	0.052
	R^2	0.95	0.94	0.96	0.96		
MS +PFA + TBAB	k (min^{-1})	6.70×10^{-3}	9.80×10^{-3}	1.22×10^{-2}	2.02×10^{-2}	29.52	805.93
	R^2	0.95	0.96	0.97	0.97		
US + PFA + TBAB	k (min^{-1})	1.80×10^{-2}	4.26×10^{-2}	3.67×10^{-2}	3.59×10^{-2}	16.43	15.96
	R^2	0.92	0.97	0.98	0.95		

Experimental Category	Thermodynamic Property											
	ΔH (kJ/mol)				$-\Delta S$ (kJ/mol K)				ΔG (kJ/mol)			
	Temperature											
B. Thermodynamic analysis	303 K	313 K	323 K	333 K	303 K	313 K	323 K	333 K	303 K	313 K	323 K	333 K
A1. MS + PFA	36.22	36.13	36.05	35.97	0.22	0.21	0.22	0.22	101.96	102.92	105.57	108.34
A2. US + PFA	3.44	3.36	3.28	3.91	0.31	0.31	0.31	0.31	98.23	100.72	104.14	107.55
B1. MS +PFA + TBAB	27.00	26.91	26.83	26.75	0.23	0.23	0.23	0.23	97.12	99.47	102.15	104.00
B2. US + PFA + TBAB	13.91	13.82	13.74	13.67	0.27	0.26	0.27	0.27	94.68	95.65	99.23	102.40

Notation: k – pseudo–1st order kinetic constant (min^{-1}), R^2 – regression coefficient, E_a – activation energy (kJ/ mol), A – frequency factor or pre–exponential factor (mol /L–min).

Table 3. Summary of the simulations of cavitation bubble dynamics[#]

	Toluene	
	Air bubble R_o = 5 μm P_o = 101.3 kPa	Air bubble R_o = 5 μm P_o = 162 kPa
Species	T_{max} = 4835 K P_{max} = 961 MPa V_{turb} = 0.15 m/s P_{AW} = 30.20 MPa	T_{max} = 1076 K P_{max} = 80.25 bar V_{turb} = 0.014 m/s P_{AW} = 0.69 bar
	x_{N2} = 0.79 x_{O2} = 0.21 x_{TOL} = 2.77E–6	x_{N2} = 0.79 x_{O2} = 0.21 x_{TOL} = 4.91E–7
Equilibrium mole fraction		
N_2	7.11E–1	7.90E–1
O_2	1.25E–1	2.10E–1
O	2.05E–2	–
O_3	3.80E–5	–
N	1.91E–4	–
N_3	3.82E–6	–
NO	1.41E–1	7.60E–5
NO_2	2.27E–3	2.18E–5
NO_3	1.64E–6	–
N_2O_3	1.14E–6	–
N_2O	7.41E–4	–
CO	1.23E–6	–
CO_2	2.18E–6	–
OH	3.37E–6	–
H_2O	–	–
HO_2	–	–
H_2O_2	–	–
HNO_2	–	–

– Data reproduced from **ref**. [14]

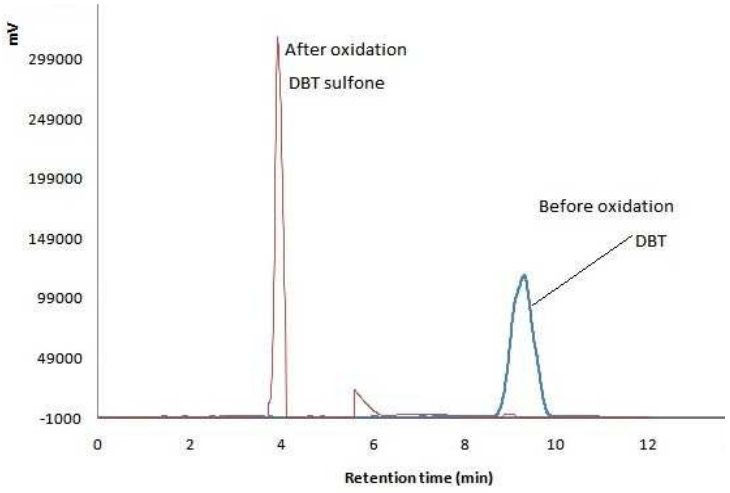

Fig. 1: HPLC Chromatograph of reaction mixture before and after treatment for oxidant system: Performic acid + TBAB as phase transfer agent

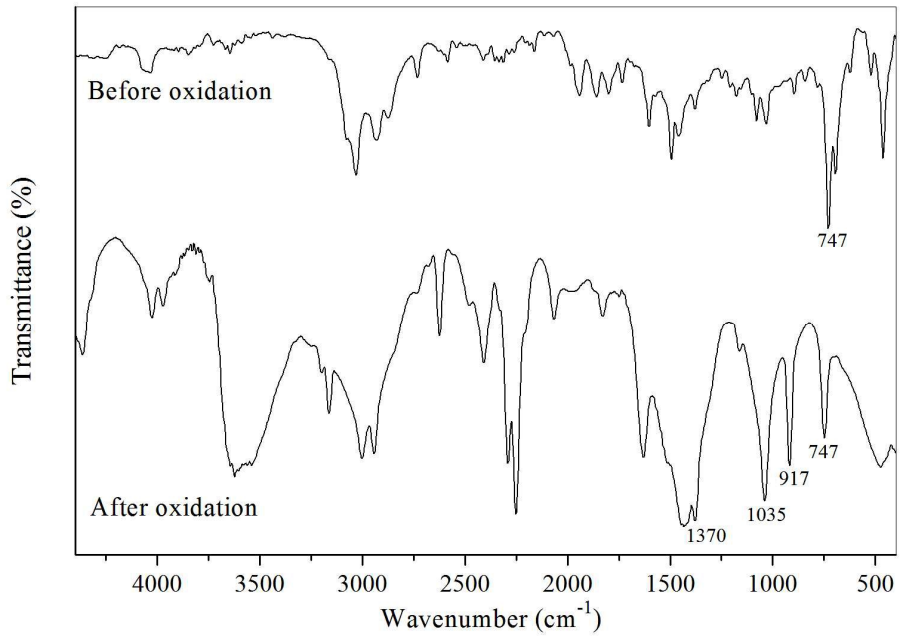

Fig. 2: Comparison of the FTIR spectra of before and after oxidation reaction (protocol: experimental category B, *i.e.* ultrasound treatment with oxidant performic acid in presence of TBAB as phase transfer agent)

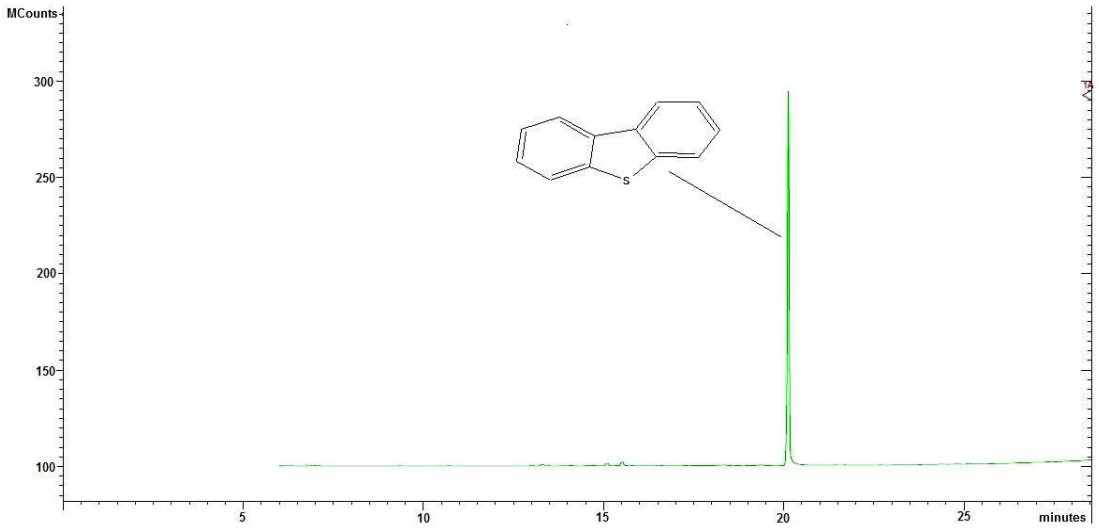

(A)

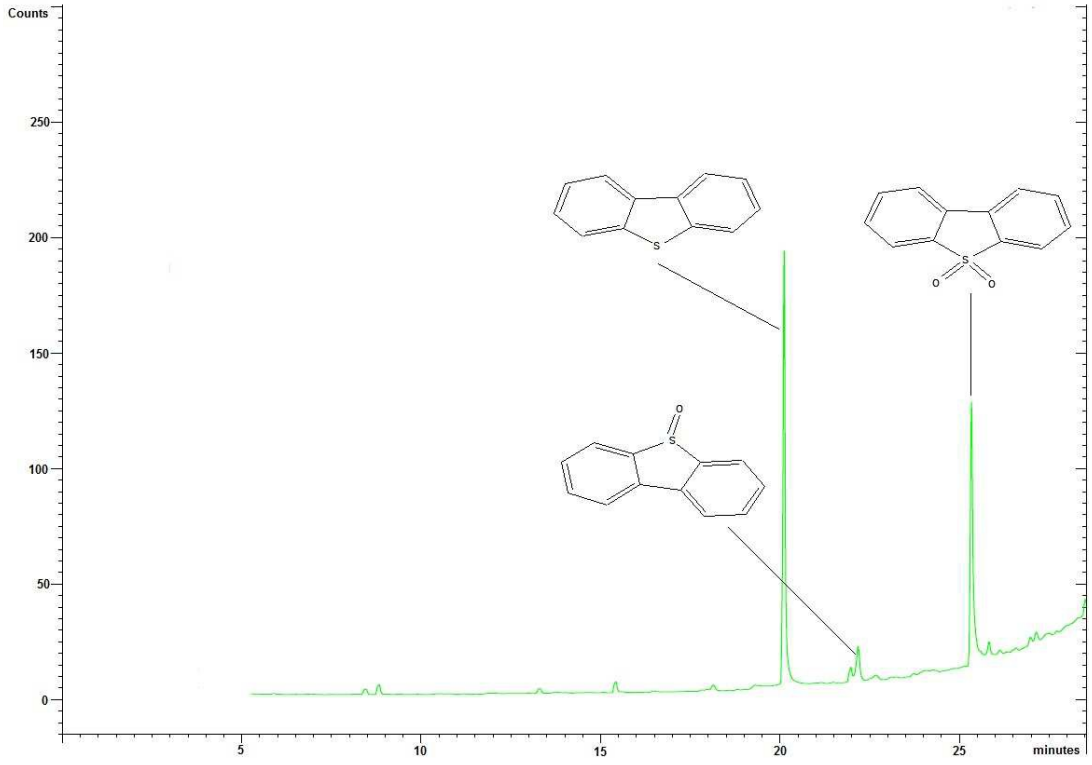

(B)

Fig. 3: Total ion chromatogram of the reaction mixture in experimental category B (protocol: ultrasound treatment with oxidant performic acid in presence of TBAB as phase transfer agent). (A) Initial (before reaction) chromatogram; (B) Final (after oxidation reaction) chromatogram

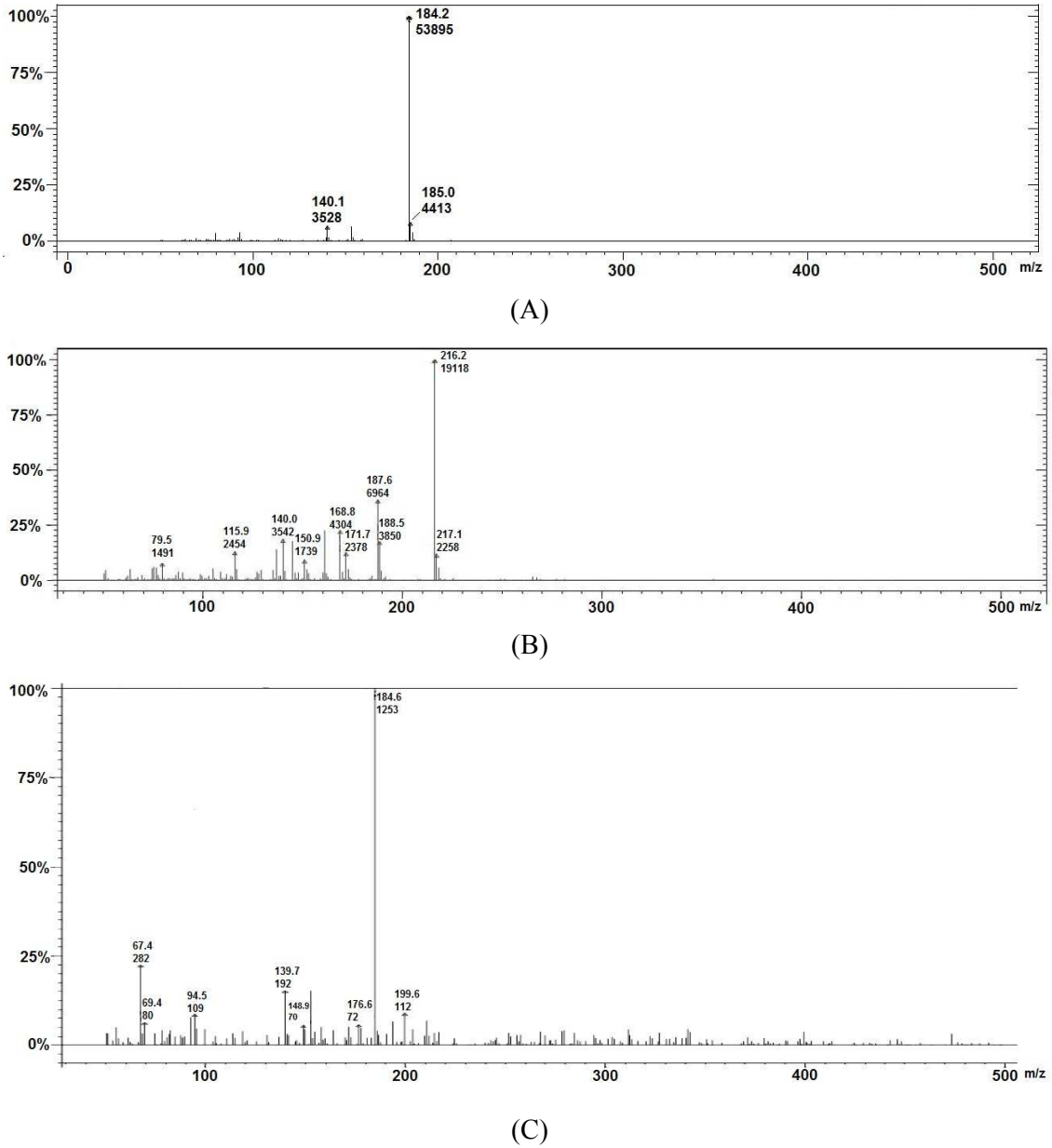

Fig. 4: Mass spectrum of reaction mixture after treatment in experimental category B (protocol: ultrasound treatment with oxidant performic acid in presence of TBAB as phase transfer agent). **(A)** Mass spectrum of DBT; **(B)**: Mass spectrum of DBT sulfone; **(C)** Mass spectrum of DBT sulfoxide

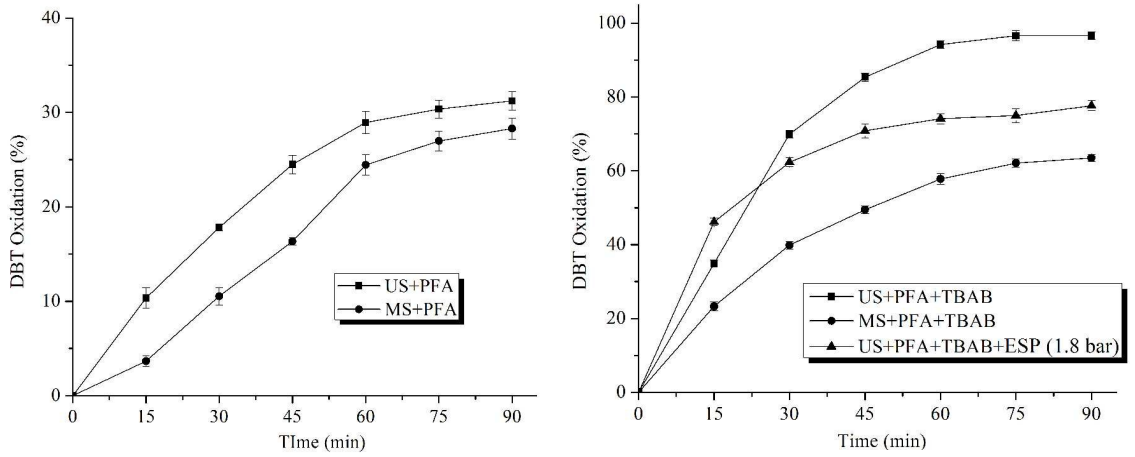

(A) (B)

Fig. 5: Time profiles of DBT oxidation in different experimental categories. (A) Categories A1 (MS + PFA) and A2 (US + PFA). (B) Categories B1 (MS + PFA + TBAB), B2 (US + PFA + TBAB) and C1 (US + PFA + TBAB at elevated static pressure). Temperature of reaction: Mechanically stirred (MS) systems = 333 K, Ultrasound-assisted (US) systems = 313 K.